7th Australasian Hydraulics and
Fluid Mechanics Conference,
Brisbane, 18-22 August, 1980

Double-Diffusive Convection with a Nonlinear Equation of State

T.J. McDOUGALL

Research School of Earth Sciences, The Australian National University, A.C.T.

SUMMARY In recent years it has been realized that double-diffusive convection plays an important role in the mixing of temperature and salinity in the world's oceans. In this paper we investigate the convection which occurs in two mixed layers separated by a sharp fluid interface when there are two different mechanisms which can cause convection; firstly the diffusive type of double-diffusive convection and secondly the cabbeling instability. The term cabbeling describes the convection that can occur when a mixture of two oceanic water masses is more dense than both of the parent water masses. Because of the nonlinearity of the equation of state, vigorous convection is driven in the lower layer while the convective activity in the upper layer is reduced. This causes an entrainment of fluid from the upper layer into the lower layer and so contributes to the rate of change of layer properties in addition to those changes caused by the symmetrical fluxes of double diffusive convection.

1 INTRODUCTION

The term cabbeling has been used to describe the convection caused by the nonlinearity of the equation of state of sea-water. The sinking which occurs when horizontally adjacent water masses mix and produce denser water is an important process in the formation of Antarctic Bottom Water (Foster and Carmack 1976a) and this process has long been known as cabbeling. Recently the term cabbeling has been used by Foster (1972) and Foster and Carmack (1976b) to describe the convection which occurs between vertically adjacent water masses (separated by a horizontal interface) when a mixture of the water masses is denser than the lower layer. We point out here that when this situation occurs with sea-water, the temperature and salinity are distributed so that double diffusive convection also operates between the layers and we show that this double-diffusive convection profoundly effects the behaviour of the system. Instead of observing convective motions only in the lower layer we see active (double-diffusive) convection in both layers. The level of convective activity is observed to be greater in the lower layer than in the upper layer and this together with the reduced static stability at the lower edge of the interface causes the interface to migrate upwards as the lower layer grows at the expense of the upper layer. This vertical interface migration occurs not only when the effects of the nonlinear equation of state are large enough so that normal cabbeling is possible, but also for less severe deviations from a linear equation of state.

2 CONSERVATION OF MASS, SOLUTE AND ENTHALPY

Consider a layer of cool fresh water overlying a layer of warm salty water. We define the fluxes of heat F_h, of salt F_s and of water F_w as positive upwards. The direct entrainment of upper layer fluid into the lower layer by energetic turbulent eddies is parameterized by the entrainment velocity U_e. The conservation of the masses of the layers and of the mass of solute in the upper and lower layers gives

$$d(\rho_u H_u)/dt = -U_e\rho_u + F_w + F_s \quad , \qquad (1a)$$

$$d(\rho_\ell H_\ell)/dt = U_e\rho_u - F_w - F_s \quad , \qquad (1b)$$

$$d(\rho_u H_u S_u)/dt = + F_s - U_e\rho_u S_u \quad , \qquad (2a)$$

$$d(\rho_\ell H_\ell S_\ell)/dt = - F_s + U_e\rho_u S_u \quad . \qquad (2b)$$

The subscripts u and ℓ refer to the upper and lower layers respectively, ρ is the density and S is the salinity. The layer depths H_u and H_ℓ cannot be measured very accurately (either in the laboratory or in the ocean) compared with the precision which is readily achieved in the measurements of temperatures and salinities. It is convenient to define the "apparent" fluxes of salt and enthalpy as being the rate of change of the salinity S or the specific enthalpy h in a layer, multiplied by the mass of the layer per unit interface area (ρH). From (1) and (2), the apparent fluxes of salt are

$$\rho_u H_u dS_u/dt = + F_s - S_u[F_w+F_s] \qquad (3a)$$

$$\rho_\ell H_\ell dS_\ell/dt = -F_s+S_\ell[F_w+F_s]-U_e\rho_u\Delta S \qquad (3b)$$

where ΔS is $S_\ell - S_u$. It is obvious that $-\rho_u H_u dS_u/dt$ is not equal to $\rho_\ell H_\ell dS_\ell/dt$ even in the absence of direct entrainment (i.e. $U_e=0$). but in every previous study of double-diffusive convection, the presence of the $[F_w+F_s]$ terms in (3) has gone undiscovered and the apparent flux of salt has been put equal to F_s. This neglect can lead to serious errors for a sugar-salt finger interface (McDougall (1980). Due tc lack of space here we cannot derive the accurate conservation equations for enthalpy (see McDougall (1980) but we quote the resultant apparent fluxes of enthalpy

$$\rho_u H_u dh_u/dt = +F_h+F_s(h_s-h_u)+F_w(h_w-h_u) \qquad (4a)$$

$$\rho_\ell H_\ell dh_\ell/dt = -F_h-F_s(h_s-h_\ell)-F_w(h_w-h_\ell)-U_e\rho_u\Delta h. \qquad (4b)$$

h_s is the differential heat of solution of sea-salt, h_w is the partial specific enthalpy of pure water

in a sea-water solution and $\Delta h = h_\ell - h_u$.

The flux of heat across a diffusive interface is larger than the flux of salt (in density units) and so we choose the asymmetric apparent flux of enthalpy divided by the mean apparent flux of enthalpy as the most appropriate nondimensional measure (called the entrainment parameter $\tilde{E}$) of the interface migration. We have then

$$\tilde{E} \equiv \frac{\rho_\ell H_\ell dh_\ell/dt + \rho_u H_u dh_u/dt}{\rho_\ell H_\ell dh_\ell/dt - \rho_u H_u dh_u/dt}$$

$$= \frac{1 - \frac{\rho_u H_u}{\rho_\ell H_\ell}(-\frac{dh_u}{dh_\ell})}{1 + \frac{\rho_u H_u}{\rho_\ell H_\ell}(-\frac{dh_u}{dh_\ell})} \qquad (5)$$

$$= \frac{(U_e\rho_u - F_w - F_s)\Delta h}{2\{F_h + F_s(h_s - h_u) + F_w(h_w - h_u)\} + (U_e\rho_u - F_w - F_s)\Delta h}.$$

We take the "expansion coefficients" for temperature T and salinity S to be defined by $\alpha = -\frac{1}{\rho}\frac{\partial\rho}{\partial T}$ and $\beta = \frac{1}{\rho}\frac{\partial\rho}{\partial S}$. The mean apparent flux of buoyancy (B_m) into the upper and lower layers is then given by

$$2\frac{\rho_o}{g}B_m = H_\ell d\rho_\ell/dt - H_u d\rho_u/dt \qquad (6)$$

$$= [\frac{\alpha_u}{C_u}\rho_u H_u \frac{dh_u}{dt} - \frac{\alpha_\ell}{C_\ell}\rho_\ell H_\ell \frac{dh_\ell}{dt}] + [\beta_\ell \rho_\ell H_\ell dS_\ell/dt - \beta_u \rho_u H_u dS_u/dt]$$

where C is the specific heat and we have assumed that the specific enthalpy of sea-water is a function only of temperature. The most sensible choice for the buoyancy flux ratio R_f is the ratio of the two bracketed terms in (6) which leads to equation (7) (see bottom of page).

3 DIMENSIONAL ANALYSIS AND THE SIMPLIFICATIONS FOR SEA-WATER

A given flux of heat across an interface gives rise to different buoyancy fluxes in the upper and lower layers because the expansion coefficient due to temperature, α, is different in the two layers. This difference in the buoyancy fluxes drives different levels of convective activity in the two layers which in turn may cause preferential entrainment of fluid from one layer into the other. The extent of this asymmetric entrainment depends on the parameter $\frac{\alpha_\ell - \alpha_u}{\alpha_\ell + \alpha_u}$.

We need to also define a parameter which represents the static gravitational stability of a horizontal fluid interface with respect to mixing of the upper and lower fluids. Figure 1 shows some density versus mixture ratio curves for mixtures of two sea-water masses at atmospheric pressure. The straight line on figure 1 is the result with a linear equation of state. We choose the maximum value of the difference in density ($\delta\rho$max) between the actual equation of state and a linear equation of state as the most relevant physical parameter describing the importance of the nonlinearity of the equation of state. The appropriate nondimensional parameter is then defined as $\tilde{\delta} \equiv 4\frac{\delta\rho\max}{\Delta\rho}$ and we refer to $\tilde{\delta}$ as the cabbeling parameter. Cabbeling is conventionally thought to be possible only when the density of a mixture is denser than ρ_ℓ, that is, when the curves in figure 1 have a maximum. Later in this section we show that this occurs for $\tilde{\delta} > 1{\cdot}0$.

Dimensional arguments for double-diffusive convection with a linear equation of state show that the buoyancy flux ratio R_f is a function of the stability ratio R_ρ, the Prandtl number ν/κ_T and the ratio of the molecular diffusivities $\tau = \kappa_S/\kappa_T$ (see Turner (1973) chapter 8). When the equation of state is nonlinear we have two extra nondimensional parameters: $\frac{\alpha_\ell - \alpha_u}{\alpha_\ell + \alpha_u}$ which represents the difference between the convective activity in the two layers and $\tilde{\delta}$ which represents the stability of the interface due to the mixing of the two water masses. That is, we have

$$R_f = f(R_\rho, \nu/\kappa_T, \kappa_S/\kappa_T, \frac{\alpha_\ell - \alpha_u}{\alpha_\ell + \alpha_u}, \tilde{\delta}) .$$

Both $\frac{\alpha_\ell - \alpha_u}{\alpha_u + \alpha_\ell}$ and $\tilde{\delta}$ are caused by the nonlinearity of the equation of state and so for a given equation of state these two parameters are related. The equation of state of sea-water can be approximated by an expression quadratic in the temperature. By expressing the temperature and salinity of a fluid mixture as a function of the mixture ratio and using the quadratic equation of state, it is straightforward to show that the conditions under which cabbeling is normally assumed to occur correspond to $\tilde{\delta} > 1.0$ and that $\tilde{\delta}$, $\frac{\alpha_\ell - \alpha_u}{\alpha_\ell + \alpha_u}$ and R_ρ are related by

$$\tilde{\delta} = \frac{\alpha_\ell - \alpha_u}{\alpha_\ell + \alpha_u} \cdot \frac{1}{(R_\rho - 1)} \qquad (8)$$

where R_ρ is the stability ratio which is familiar from normal double-diffusive convection. For the present purposes R_ρ can be taken as $\beta_m \Delta S / \frac{\alpha_m}{C_m}\Delta h$, where β_m, α_m and C_m are evaluated at $T_m = \frac{1}{2}(T_u + T_\ell)$ and $S_m = \frac{1}{2}(S_u + S_\ell)$.

$$R_f = \frac{dS_\ell}{dT_\ell} \frac{[\beta_\ell + \beta_u \cdot \frac{\rho_u H_u}{\rho_\ell H_\ell}(-\frac{dS_u}{dS_\ell})]}{[\frac{\alpha_\ell}{C_\ell} + \frac{\alpha_u}{C_u} \cdot \frac{\rho_u H_u}{\rho_\ell H_\ell} \cdot (-\frac{dT_u}{dT_\ell})]} \qquad (7)$$

$$= \frac{F_s(\beta_\ell + \beta_u) + U_e\rho_u\beta_\ell\Delta S - [F_w + F_s](\beta_\ell S_\ell + \beta_u S_u)}{F_h(\frac{\alpha_\ell}{C_\ell} + \frac{\alpha_u}{C_u}) + U_e\rho_u\frac{\alpha_\ell}{C_\ell}\Delta h + F_s[\frac{\alpha_\ell}{C_\ell}(h_s - h_\ell) + \frac{\alpha_u}{C_u}(h_s - h_u)] + F_w[\frac{\alpha_\ell}{C_\ell}(h_w - h_\ell) + \frac{\alpha_u}{C_u}(h_w - h_u)]}$$

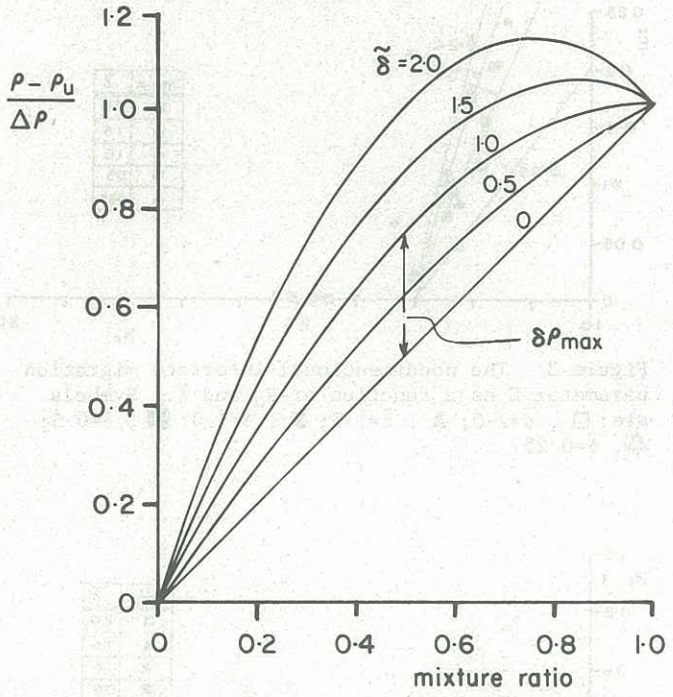

Figure 1 The density of mixtures of two sea-water masses in varying proportions. $\delta\rho_{max}$ is illustrated for the $\tilde{\delta}$ = 1·0 curve. The curve $\tilde{\delta}$ = 0 is a straight line and it represents a linear equation of state.

Now because $\frac{\alpha_\ell-\alpha_u}{\alpha_\ell+\alpha_u}$ and $\tilde{\delta}$ are related, the dimensional analysis leads us to expect $R_f = f(R_\rho, \tilde{\delta})$ for a given set of molecular properties ν, κ_T and κ_s. Other nondimensional properties such as $\tilde{E}$ are also expected to be functions of R_ρ and $\tilde{\delta}$ only.

4 EXPERIMENTAL RESULTS

The experiments were conducted in a perspex tank with a rectangular cross-section 575mm x 100mm and the depths of both the upper and lower layers were initially 225mm. The tank was constructed so that a thin sheet (1.5mm thick) of polypropylene which initially separated the two fluid layers could be slid out through the front face of the tank, thereby bringing the upper and lower layers into contact and so starting the experiment. This polypropylene sheet was sealed above, below and at both sides by O-ring material to form a perfect fluid seal. Copper resistance wire wound on 6mm O.D. perspex rods provided a good method of measuring the average temperatures along the whole length of the mixed layers. The salinities of the mixed layers were measured by periodically withdrawing samples from each layer.

We conducted a series of seven experiments with diffusive heat-salt interfaces and table I shows the details of the starting conditions of these experiments. The most striking feature of these experiments was the upward migration of the interface and this was especially obvious in the experiments with large initial cabbeling parameter $\tilde{\delta}$. The fluid motions in the tank were observed on a shadowgraph and one layer was dyed with food colouring. Colour photographs and a movie provided visual evidence of the interface movement during the experiment.

Figure 2(a) is a shadowgraph photograph taken 42 seconds after the start of the experiment on 3 September 1979. Fluid samples taken at this time showed that the stability ratio R_ρ was 1·23, the cabbeling parameter was 4·73 and the density difference between the layers $\Delta\rho$ was $0{\cdot}87\times10^{-3}$ g/ml. The thick black horizontal line across the centre of the photograph is where the polypropylene sheet is located and it marks the initial position of the fluid interface. Figure 2(b) shows a later stage of the same experiment, almost 15 minutes after the start of the experiment. The stability ratio R_ρ had increased to 1·81, the cabbeling parameter $\tilde{\delta}$ had decreased to 0·76 and the density difference had increased to $1{\cdot}92\times10^{-3}$gm/ml. Visual observations of the shadowgraph during the experiments showed that the amount of convective activity was greater in the lower layer than in the upper layer. The reason for the greater convective activity in the lower layer is readily seen from the following simple argument. For given fluxes of heat F_h and salt F_S across a diffusive interface, the buoyancy flux in the lower layer is $\frac{g}{\rho_o}(\frac{\alpha_\ell}{C_\ell}F_h - \beta_\ell F_S)$ and the buoyancy flux in the upper layer is $\frac{g}{\rho_o}(\frac{\alpha_u}{C_u}F_h - \beta_u F_S)$.

TABLE I

DETAILS OF THE INITIAL CONDITIONS OF THE EXPERIMENTS

Date	Initial R_ρ	Initial $\tilde{\delta}$	Initial T_u (°C)	Initial T_ℓ (°C)	Initial S_u (‰)	Initial S_ℓ (‰)	Initial $\Delta\rho$ (10^{-3} gm/ml)
22 Aug. 79	1.22	3.64	2.35	29.27	15.50	23.72	1.15
3 Sep. 79	1.12	8.76	2.22	29.78	0.05	6.47	0.54
18 Sep. 79	1.24	2.19	2.09	9.95	22.83	24.05	0.19
25 Sep. 79	1.28	2.72	5.11	13.36	0.05	1.10	0.18
15 Oct. 79	1.33	0.84	18.57	31.58	0.03	6.02	1.11
17 Oct. 79	1.22	1.47	16.87	31.60	0.04	6.04	0.81
25 Oct. 79	1.26	1.31	15.50	30.39	0.04	6.01	0.95

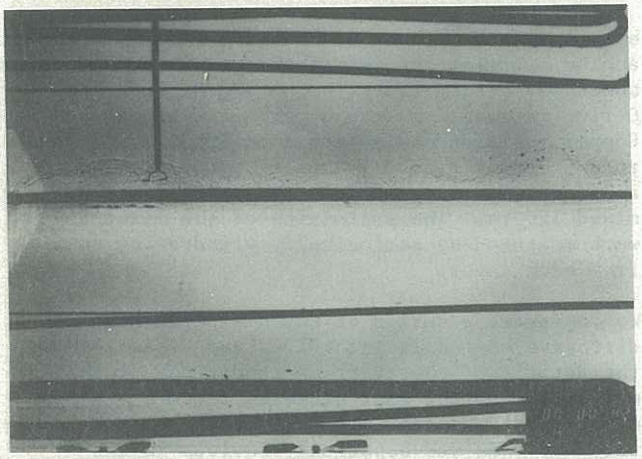

(a)

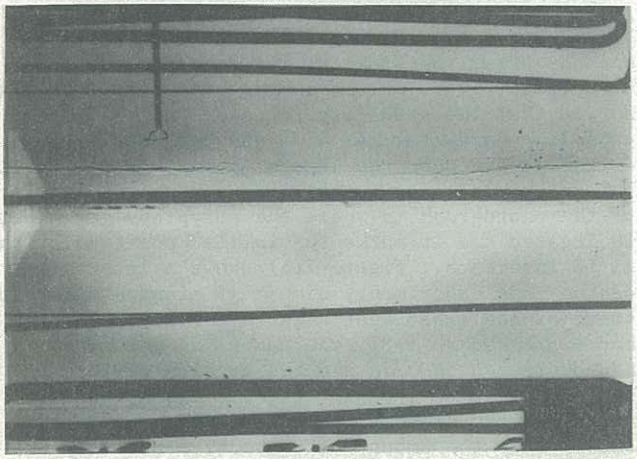

(b)

Figure 2 Two shadowgraphs of a cabbeling diffusive heat sea-salt interface. Figure (a) is 42 seconds after the start of the experiment and figure (b) is 15 minutes after the start.

Here ρ_o is a reference density, g is the gravitational acceleration and C is the specific heat. We have neglected here any effects of the flux of water F_w and the entrainment velocity U_e on the buoyancy fluxes. The upper layer is cooler than the lower layer and so $\frac{\alpha_u}{C_u}$ is less than $\frac{\alpha_\ell}{C_\ell}$ while β_u and β_ℓ are very nearly equal. This means that the buoyancy flux in the lower layer is greater than in the upper layer and we expect this larger buoyancy flux to drive more energetic convective turbulence in the lower layer.

Figure 3 shows the experimental data for the nondimensional entrainment parameter $\tilde{E}$ plotted against the stability ratio R_ρ for several values of the cabbeling parameter $\tilde{\delta}$. These data were calculated from the middle line of (5) by plotting h_u against h_ℓ, drawing a smooth curve through the data points and then measuring the derivative dh_u/dh_ℓ of this curve. The estimated accuracy of each of these values of $\tilde{E}$ is about ±15% and the R_ρ values are known to ±0.03. There is no clear dependence of the data in figure 3 on $\tilde{\delta}$ but there is a strong dependence on R_ρ. The four line segments are from a model which we do not discuss here.

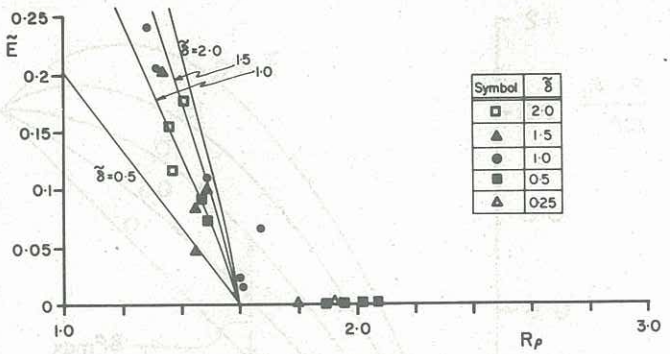

Figure 3 The nondimensional interface migration parameter E as a function of R_ρ and $\tilde{\delta}$. Symbols are: □, $\tilde{\delta}$=2·0; ▲, $\tilde{\delta}$=1·5; ●, $\tilde{\delta}$=1·0; ■, $\tilde{\delta}$=0·5; △, $\tilde{\delta}$=0·25.

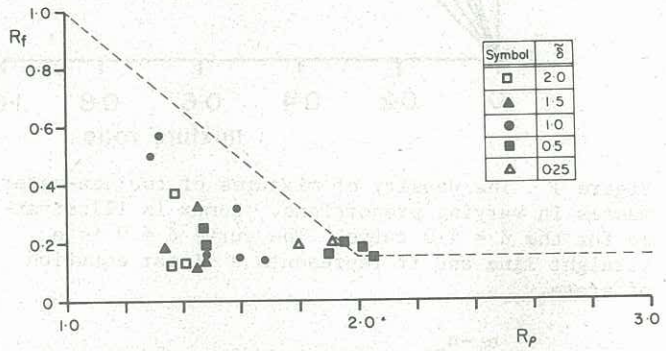

Figure 4 The buoyancy flux ratio R_f as a function of R_ρ and $\tilde{\delta}$. The key to the different symbols is in the caption of figure 3.

The flux ratio R_f was calculated from the upper line of (7) and figure 4 shows our experimental data for a cabbeling diffusive interface. Again there is a strong dependence on R_ρ but no clear pattern with $\tilde{\delta}$. The dashed line on figure 4 is the accepted wisdom of the way R_f depends on R_ρ when the equation of state can be taken as linear (Turner (1965)), however there has been some suggestion in the literature (Crapper (1975)) that the flux ratio R_f may not rise above 0·15 until R_ρ is less than 1·6, at least for small temperature and salinity differences between the layers.

The nondimensional asymmetric apparent buoyancy flux ($\tilde{B}a$) is given by

$$\tilde{B}a = \frac{H_\ell d\rho_\ell/dt + H_u d\rho_u/dt}{H_\ell d\rho_\ell/dt - H_u d\rho_u/dt} = \frac{1 - \frac{H_u}{H_\ell}\left(-\frac{d\rho_u}{d\rho_\ell}\right)}{1 + \frac{H_u}{H_\ell}\left(-\frac{d\rho_u}{d\rho_\ell}\right)} \qquad (9)$$

and this equation shows how $\tilde{B}a$ may be evaluated by finding the slope of the ρ_u versus ρ_ℓ curve. A value of $\tilde{B}a$ of 1·0 means that the upper layer density remains steady as the lower layer density increases and a value of $\tilde{B}a$ greater than 1·0 means that the upper layer density actually *increases* with time. Figure 5 shows the experimental data of $\tilde{B}a$. The main trend of this data can be explained as being solely due to the different values of α_u and α_ℓ. The five line segments on figure 5 for $\tilde{\delta}$=0.25 to 2·0 are from a model of $\tilde{B}a$ which assumes that $\tilde{E}$ = 0, U_e = 0 so that only the variation of α with temperature makes $\tilde{B}a$ non-zero and the good agreement between the data and these lines shows that this dependence of $\tilde{B}a$ on α is indeed dominant.

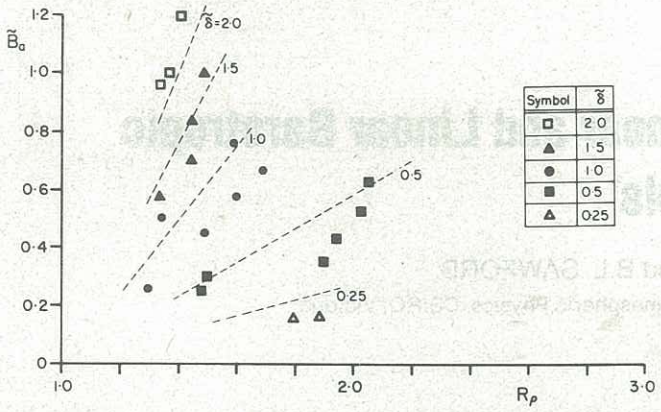

Figure 5 The nondimensional asymmetric apparent buoyancy flux $\tilde{B}a$ plotted against R_ρ for the five values of $\tilde{\delta}$ from 0·25 to 2·0.

5 CONCLUSIONS

We have elucidated the relative importance of cabbeling and double-diffusive convection. Cabbeling is normally thought to be possible only when the density of a mixture of two water masses is denser than both of the original water masses. This condition corresponds to the cabbeling parameter ($\tilde{\delta}$) being greater than unity. Our experimental results for the nondimensional interface migration ($\tilde{E}$) show that the entrainment across an interface increases monotonically as the nonlinearity of the equation of state increases and no sudden change in behaviour occurs at $\tilde{\delta} = 1{\cdot}0$. These results have been explained in terms of the increased double-diffusive convective activity in the lower layer and the smaller static gravitational stability at the lower edge of the interface: both of these effects being due to the nonlinear equation of state. Our results can now be used to determine the interface movement and total downward fluxes of properties in the deep Weddell Sea T and S profiles of Foster and Carmack (1976b) and Middleton and Foster (1980) where a series of interfaces with $R_\rho \simeq 1{\cdot}08$ and $\tilde{\delta} \simeq 1{\cdot}0$ have been observed.

ACKNOWLEDGEMENTS

The experimental apparatus was very ably designed and constructed by Derek Corrigan and I wish to thank Ross Wylde-Browne and Derek Corrigan for assistance with the experiments. During the course of this work I have been supported by a Queen's Fellowship in Marine Science.

REFERENCES

CRAPPER, P.F. (1975). Measurements across a diffusive interface. Deep-Sea Research, 22, 537-545.

FOSTER, T.D. (1972). An analysis of the Cabbeling Instability in Sea Water. Journal of Physical Oceanography, 2, 294-301.

FOSTER, T.D. and CARMACK, E.C. (1976a). Frontal zone mixing and Antarctic Bottom Water formation in the southern Weddell Sea. Deep-Sea Research, 23, 301-317.

FOSTER, T.D. and CARMACK, E.C. (1976b). Temperature and salinity structure in the Weddell Sea. Journal of Physical Oceanography, 6, 36-44.

McDOUGALL, T.J. (1980). Double-Diffusive Convection with a nonlinear equation of state. Part I, The accurate conservation of properties across an interface. Submitted to Deep-Sea Research.

MIDDLETON, J.H. and FOSTER, T.D. (1980). Fine-structure measurements in a temperature compensated Halocline. Journal of Geophysical Research, to appear.

TURNER, J.S. (1965). The coupled transports of salt and heat across a sharp density interface. International Journal of Heat and Mass Transfer, 8, 759-767.

TURNER, J.S. (1973). Buoyancy effects in fluids. Cambridge University Press. 367pp.